

**K. Bria<sup>1</sup>, M. Ait El Fqih<sup>1,\*</sup>, R. Jourdani<sup>2</sup>, L. Jadoual<sup>2</sup>, A. Kaddouri<sup>2</sup>**<sup>1</sup>Laboratory of Artificial Intelligence & Complex Systems Engineering,

National Graduate School of Arts and Crafts, Hassan II University, Casablanca, Morocco

<sup>2</sup>Laboratory of Materials, Energy, and Environment, Cadi Ayyad University, Marrakech, Morocco

\*Corresponding author: m.aitelfqih@gmail.com

**EFFECTS OF LITHIUM INSERTION INTO VANADIUM PENTOXIDE THIN FILMS.  
CONTINUUM RADIATION STUDY**

Optical emission of  $\text{Li}_{x(x=0.2,0.7,1.2)}\text{V}_2\text{O}_5$  has been studied during 5 keV  $\text{Kr}^+$  ions bombardment. Continuous luminescence was observed in a broad wavelength range between 280 and 340 nm. Generally, the emission intensity was influenced by the quantities of lithium giving rise to transient effects as well as an increase in the line intensity. The experimental results suggest that the continuum emission depends on the nature of surface interaction between lithium and vanadium pentoxide and is very probably related to its electronic structure.

*Keywords:* sputtering, sol-gel, optical-emission, vanadium pentoxide, intercalation and deintercalation.

**1. Introduction**

Nowadays, lithium-ion batteries are the most applied technology in many factories such as hybrid electric vehicles [1], various portable electronic devices [2], and emerging smart grids [3]. The use of batteries is growing due to the environmental issues caused by the depletion of fossil energy resources.

However, many studies have been explored to improve the performance of vanadium-based electrode materials. In these topics, the performance and working mechanism of amorphous electrode materials are far less understood.

Moreover, it is well known that the intercalation of lithium into  $\text{V}_2\text{O}_5$  layers leads to the occupation of originally empty conduction band states corresponding to 3d-shell. During the insertion of lithium, the shift of Fermi level and formation of surface dipole has been observed in amorphous  $\text{Li}_x\text{V}_2\text{O}_5$  [4] and  $\text{Na}_x\text{V}_2\text{O}_5$  [5] deposited by the physical vapor deposition technique.

Several recent studies have implemented vanadium oxides as the battery [6]. Zheng et al. prepared  $\text{V}_2\text{O}_5$  as the battery-type electrode for hybrid supercapacitors [7]. They indicate that the increasing complexity of the structure leads to lower specific capacitance because of the higher degree of electrode polarization and higher resistance. Wang et al. synthesized  $\text{V}_2\text{O}_5$  hollow spheres with triple double-walled shells. They show improved electrochemical performance compared to single-shelled  $\text{V}_2\text{O}_5$  hollow microspheres as electrode materials for lithium-ion batteries [8]. Han et al. [9] found that Fe doping enhanced  $\text{Li}^+$  diffusivity arising from the expansion of the 1D channel in the polyanion structure of  $\text{LiCoPO}_4$ .

Li et al. [10] observed that the electrical conductivity of  $\text{LiCoPO}_4$  increased three orders of magnitude via coating with uniform carbon film. Covering the  $\text{LiCoPO}_4$  cathode with a thin layer of  $\text{Al}_2\text{O}_3$  could greatly alleviate the capacity fading.

Generally, continuum emission observed in front of transition metal targets is believed to arise from excited atom clusters (including diatomic and triatomic) ejected from the solid surface in the sputtering process [11, 12]. The continuum radiation observed in the case of transition metals gives rise to a broadband continuum emission which is observed spatially at distances of a few millimeters in front of the target [13, 14]. The phenomenon depends on the presence of oxygen at the target surface and the collective deactivation of 3d-shell electrons remains a possible source. According to these authors, the continuum radiation is observed in the case of clean titanium and clean vanadium. It is found to be enhanced by the presence of oxygen, probably due to chemisorption. This enhancement can reach respectively a factor of 2 and 5 for titanium and vanadium.

In the present work, we present the results of an experimental study that highlights the continuum radiation spectra during 5  $\text{Kr}^+$  ion beam sputtering of  $\text{Li}_{x(x=0.2,0.7,1.2)}\text{V}_2\text{O}_5$  and vanadium pentoxide. To elucidate the origin of the continuum, we re-recorded the spectra of these targets under the same conditions of bombardment, spatially at the base pressure of  $10^{-7}$  Torr. The effect of lithium insertion in vanadium pentoxide is discussed.

## 2. Materials and experimental details

### 2.1. Materials

Thin films of  $V_2O_5$  were prepared by sol-gel using the spin-coating method described in reference [15].  $V_2O_5$  soil was prepared by dissolving  $V_2O_5$  powder with a solution of 15 %  $H_2O_2$  under vigorous stirring. The layers were obtained by spin coating on a glass substrate of indium tin oxide which is then rotated at a speed of 2400 rev/min to a film thickness of 216 nm. The samples were subsequently undergoing a heat treatment at 150 °C for 1 h. Electrochemical measurements are carried out in a cell containing  $V_2O_5$  film as a working electrode, a platinum electrode against a saturated calomel electrode (SCE) as a reference electrode, and a 1M solution of  $LiClO_4$  in propylene carbonate as the electrolyte. Samples analyzed by the technical SIPS are four thin layers of  $V_2O_5$ : gross; polarized - 400 mV/(colored blue) and bleached to a polarization potential of 1200 mV/SCE.

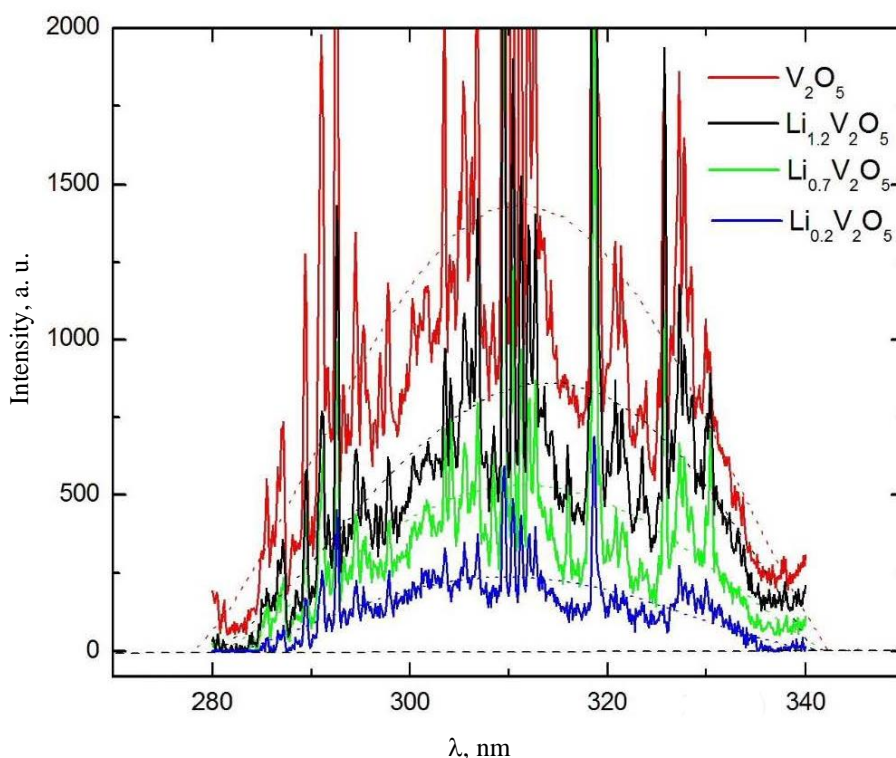
### 2.2. Experimental details

The setup used in this work is a part of SIPS installed in our laboratory and described previously [16 - 18]. Briefly,  $Kr^+$  ions with energies of 5 keV were produced by electron impact on Kr gas (of 99,998 % purity) in the plasma source. The ion beam is focused on a target mounted inside an ultra-high vacuum chamber. Vacuum is established by means of

two turbomolecular pumps of 50 and 200 l/s capacities, respectively. In the absence of ionic bombardment, the residual pressure near the sample is less than  $10^{-7}$  Torr. Prior to the start of each measurement, the targets were cleaned in situ by ion beam sputtering. The ion beam current was measured directly on the sample or by a Faraday cup placed behind the target, in the direction of the ion beam. The sample holder can rotate to change the angle of incidence between the ion beam and the normal to the sample surface and translate for consecutive analysis of several samples. The cross-section was 0.95 mm<sup>2</sup> given a fluence of  $3.3 \cdot 10^8$  ion/mm<sup>2</sup>. The incident angle was 60°. This angular position from the normal to the surface maximizes the sputtering yield and therefore the photon yield. The emitted light was analyzed through an R320 Jobin - Yvon monochromator equipped with 1800 groves/mm holographic grating using a 400  $\mu$ m slit width. Hamamatsu 4220P photomultiplier is used to explore the wavelength range and a micro-computer is used with the PRISM program to control the whole detection system and to collect data.

## 3. Experimental results and discussion

Figure shows the partial optical spectrum of vanadium pentoxide and  $Li_{x(x=0.2,0.7,1.2)}V_2O_5$  bombarded by 5 keV  $Kr^+$ . These samples are sealed in a vacuum chamber and examined under the same experimental conditions (Table 1).



Photon spectrum of clean  $V_2O_5$  and  $Li_{x(x=0.2,0.7,1.2)}V_2O_5$  films bombarded by 5 keV  $Kr^+$  ions. The dotted line is the best-fit curve for the continuum radiation. (See color Figure on the journal website.)

**Table 1. Experimental conditions of recording the spectra of luminescence by SIPS**

Vacuum in the target chamber	$< 10^{-7}$ torr
Monochromator slits	400 mm
Angles of incidence	$70^\circ$
Wavelength range	200 - 300 nm
Spectral resolution	0.32 nm
Counting time	1000 ms
Sample current	0.5 - 0.6 mA
Ion's energy	5 keV

The observed spectra consist of a series of discrete lines superimposed on a broad continuum range between 280 and 340 nm. The most intense line is located at 318.7 nm and attributed to V I due to the  $3d^3 4s^2 {}^4F_{1/2} - 3d^3 4s 4p {}^4G_{1/2}$  transition.

The measured photon intensities are very higher for clean  $V_2O_5$  compared to the intercalated  $Li^+$  ions. This behavior observed is probably caused by the changes in the electronic structure of  $Li_xV_2O_5$  by the formation of surface dipole which leads to a strong shift in the Fermi level.

In the recorded spectra, the height of continuum radiation decreases with the insertion of lithium in the vanadium pentoxide. This decline can reach a factor of 2 probably due to the chemisorptions phenomenon. The solvent used during synthesis was found to play a critical role in structure formation based on the chemisorption of preferred molecules [19]. J. Yao et al. [20] focused on selected topics covering the influences of surface chemistry, crystallinity, doping, defects, and nanostructures on the lithium-ion intercalation properties and recent developments on

other metal batteries including NIBs and MIBs. For vanadium pentoxide, the collective deactivation of 3d-shell electrons appears to play a role in the emission of this radiation. Noted that this is the radiation of the knocked-out particles.

We simulated a broad-band continuum to a discrete line (see Figure). The full widths at half maximum (FWHM) (Table 2) are almost identical (37.80, 38.49, 38.15, and 38.84 for respectively  $Li_{0.2}V_2O_5$ ,  $Li_{0.7}V_2O_5$ ,  $Li_{1.2}V_2O_5$ , and clean  $V_2O_5$ ). The same phenomena were observed by Jadoual et al. [21]. They suggested that the lifetime of the continuum radiation is similarly identical in the case of titanium and Ti +  $O_2$  structures. As a result, the origin of the continuum radiation is probably the same for titanium and the structure formed in the presence of oxygen (Ti +  $O_2$ ). On the other hand, we suggest that the observed continuum radiation is due to the excited-state formation for Me-A molecules (where Me is an atom of transition metal with partly occupied d electron shells; A is an atom of reactive gas). Noted that the insertion of lithium decreases the effect of the continuum. It has been proposed that a molecule being sputtered without dissociation from the metal surface is excited beyond the region of effective electron exchange with the surface due to the transfer of kinetic energy of relative motion of the nuclei to the electron subsystem. Within the framework of this excited-state formation model, where de-excitation processes such as resonance ionization seem to be unlikely, it is possible to explain the main features observed in the continuum radiation.

**Table 2. The FWHM**

Sample	$Li_{0.2}V_2O_5$	$Li_{0.7}V_2O_5$	$Li_{1.2}V_2O_5$	$V_2O_5$
Maxima of the continuum	235 nm	535 nm	860 nm	1440 nm
FWHM	$37.80 \pm 1.5$ nm	$38.49 \pm 1.5$ nm	$38.15 \pm 1.5$ nm	$38.84 \pm 1.5$ nm

Table 3 shows the absolute intensities of observed lines in the case of the bombardment of clean  $V_2O_5$  and  $Li_{x(x=0.2,0.7,1.2)}V_2O_5$  films. The measured wavelengths of V I and V II lines and those given in the literature are denoted by  $\lambda_0$  and  $\lambda_L$ , respectively [22, 23]. The difference between  $\lambda_0$  and  $\lambda_L$  due to the calibration of the monochromator is approximately a constant value (0.2 nm). The second column lists the intensities of clean  $V_2O_5$  and  $Li_{x(x=0.2,0.7,1.2)}V_2O_5$  films. The identification of the transition responsible for the emission is given in the last column. Noted that no emission from sputtered excited atomic lithium was observed in the explored wavelength range.

The optical radiation, both from knocked-out particles and radiation arising from the luminescence of a solid body, enters the input slit of the optical

device. Noted that the surface of the target is visible from the entrance slit, so the luminescence from the surface will affect the radiation spectrum.

The origin of this type of emission is largely discussed by several authors and none of the proposed models explains experimental observations. It was first observed by Tolk, While, and Sigmund and by Van der Weg and Lugujo [24], and its origin is largely discussed. Kiyan, Gritsyna, and Fogel [25] advanced the hypothesis that it is the result of emission from sputtered atoms in which the atomic electron shell (the incomplete d-or-f-shell) is excited collectively as a result of a collision at the surface. White, Tolk, Kraus, and Van der Weg [26] as well as Kerkdijk, Schartner, and Saris [27] concluded that the emitting species are probably excited neutral metal molecules and have suggested sputtered metal di- and

**Table 3. Identification of the main lines observed in the region 280 - 340 nm during the bombardment of clean V<sub>2</sub>O<sub>5</sub> and Li<sub>x(x=0.2,0.7,1.2)</sub>V<sub>2</sub>O<sub>5</sub> films by 5 keV Kr<sup>+</sup> ions**

$\lambda_0$ , nm	$\lambda_L$ , nm	Intensity, a. u.				Transition
		V <sub>2</sub> O <sub>5</sub>	Li <sub>0.2</sub> V <sub>2</sub> O <sub>5</sub>	Li <sub>0.7</sub> V <sub>2</sub> O <sub>5</sub>	Li <sub>1.2</sub> V <sub>2</sub> O <sub>5</sub>	
289.4	289.42 V II	1231	558	462	137	3d <sup>3</sup> 4s a <sup>5</sup> F <sub>4</sub> - 3d <sup>3</sup> 4p z <sup>5</sup> D <sub>3</sub>
291.1	290.97 V II	1926	762	627	248	3d <sup>3</sup> 4s a <sup>5</sup> F <sub>5</sub> - 3d <sup>3</sup> 4p z <sup>5</sup> D <sub>4</sub>
292.6	292.49 V II	2962	1429	1002	449	3d <sup>3</sup> 4s a <sup>5</sup> F <sub>5</sub> - 3d <sup>3</sup> 4p z <sup>5</sup> F <sub>5</sub> <sup>o</sup>
294.5	294.54 V II	1335	643	432	192	3d <sup>3</sup> 4s a <sup>5</sup> F <sub>4</sub> - 3d <sup>3</sup> 4p z <sup>5</sup> F <sub>3</sub>
295.3	295.29 V II	1033	552	346	182	3d <sup>3</sup> 4s a <sup>5</sup> F <sub>3</sub> - 3d <sup>3</sup> 4p z <sup>5</sup> F <sub>2</sub>
305.5	305.72 V I	1769	1089	642	328	3d <sup>3</sup> 4s <sup>2</sup> a <sup>4</sup> F <sub>5/2</sub> - 3d <sup>3</sup> 4s4p w <sup>4</sup> F <sub>5/2</sub>
306.9	307.05 V I	2360	1437	781	362	3d <sup>3</sup> 4s <sup>2</sup> a <sup>4</sup> F <sub>7/2</sub> - 3d <sup>3</sup> 4s4p x <sup>4</sup> D <sub>7/2</sub>
308.4	308.30 V I	1093	692	642	218	3d <sup>3</sup> 4s <sup>2</sup> a <sup>4</sup> F <sub>9/2</sub> - 3d <sup>3</sup> 4s4p w <sup>4</sup> F <sub>7/2</sub>
309.5	309.41 V I	4720	2721	2213	543	3d <sup>3</sup> 4s4p x <sup>4</sup> D <sub>3/2</sub> - 3d <sup>3</sup> 4s <sup>2</sup> a <sup>4</sup> F <sub>5/2</sub>
310.4	310.18 V II	3439	1879	1209	497	3d <sup>3</sup> 4s b <sup>3</sup> G <sub>3</sub> - 3d <sup>3</sup> 4p y <sup>3</sup> G <sub>3</sub>
311.3	311.39 V IV	2338	1407	914	393	3p <sup>6</sup> 3d4d <sup>3</sup> F <sub>3</sub> - 3p <sup>6</sup> 3d5p <sup>3</sup> D <sub>2</sub>
312.1	312.22 V IV	2173	1297	804	339	3p <sup>6</sup> 3d4d <sup>3</sup> F <sub>2</sub> - 3p <sup>6</sup> 3d5p <sup>3</sup> D <sub>1</sub>
318.7	318.63 V I	6283	4832	2258	697	3d <sup>3</sup> 4s <sup>2</sup> a <sup>4</sup> F <sub>9/2</sub> - 3d <sup>3</sup> 4s4p x <sup>4</sup> G <sub>11/2</sub>
320.8	320.83 V I	1272	834	423	176	3d <sup>3</sup> 4s <sup>2</sup> a <sup>4</sup> F <sub>9/2</sub> - 3d <sup>3</sup> 4s4p x <sup>4</sup> G <sub>9/2</sub>
321.5	321.34 V I	1148	709	408	189	3d <sup>3</sup> 4s <sup>2</sup> a <sup>2</sup> G <sub>9/2</sub> - u <sup>2</sup> H <sub>11/2</sub>
327.3	327.20 V II	1841	1147	640	279	3d <sup>3</sup> 4s a <sup>3</sup> F <sub>3</sub> - 3d <sup>3</sup> 4p z <sup>3</sup> G <sub>4</sub>
327.8	327.70 V II	1643	977	601	225	3d <sup>3</sup> 4s a <sup>3</sup> F <sub>4</sub> - 3d <sup>3</sup> 4p z <sup>3</sup> G <sub>5</sub>

polymer molecules as a source of the continuum emission. Rausch et al. [28] suggested that emission from oxide molecules is responsible for the continuum. Vege [29] attributed the continua to the chemiluminescence due to oxygen reacting with the target surface. A similar chemiluminescence model of broad-band optical radiation has been proposed by Bazhin et al. [30]. Van der Weg et al. [24] observed continuum radiation from some metals during 40 keV Ar<sup>+</sup> bombardment, this included weak radiation from silicium and strong from titanium, chromium, zirconium, molibdenum, tantalum, and tungsten, and no radiation from nickel, copper, palladium, silver, and platinum. However, other authors did not report continuum radiation, under circumstances where they should have observed it according to refs, Tsong [31] did not observe continuum radiation from tantalum, vanadium, and tungsten, probably because of his optical having a very low sensitivity, Terzic et al. [32] detected only spectral lines from molybdenum under 40 keV Ar<sup>+</sup> bombardment. Stuart and Wehner [33] did not report continuum radiation from molibdenum, but the experimental conditions were different from

the setup usually used in bombardment-induced photon emission studies. Kerkow [34] bombarded, amongst others, tantalum, tungsten, molibdenum, iron, and chromium with 10 keV K<sup>+</sup> and Cs<sup>+</sup>, but did not report continuum radiation. Jensen and Veje [35] bombarded titanium with 50 keV Xe<sup>+</sup> but the observation of continuum radiation was not reported.

#### 4. Conclusion

Bombardment-induced light emission of clean V<sub>2</sub>O<sub>5</sub> and Li<sub>x(x=0.2,0.7,1.2)</sub>V<sub>2</sub>O<sub>5</sub> films were studied. The percentage of lithium insertion in the vanadium pentoxide decreases the intensities of the observed spectral lines and the continuum as well. The collective deactivation of 3d-shell electrons appears to play a role in the emission of this radiation in the case of vanadium pentoxide. The observed decreases in the insertion of lithium are probably due to a significant contribution of the Electrochemical chemisorption between lithium and vanadium pentoxide. Other experiments must be conducted to further elucidate the origin of this radiation.

#### REFERENCES

1. B.W.J. Yang et al. Classification, summarization and perspectives on state-of-charge estimation of lithium-ion batteries used in electric vehicles: A critical comprehensive survey. *J. Energy Storage* 39 (2021) 102572.
2. X. Xie et al. Low-density silk nanofibrous aerogels: fabrication and applications in air filtration and oil/water purification. *ACS Nano* 15 (2021) 1048.
3. J. Wu et al. Sodium-rich NASICON-structured cathodes for boosting the energy density and lifespan of sodium-free-anode sodium metal batteries. *InfoMat* 4 (2022) e12288.

4. Q.-H. Wu, A. Thissen, W. Jaegermann. Photoelectron spectroscopic study of Li intercalation into  $V_2O_5$  thin films. *Surf. Sci.* 578 (2005) 203.
5. Q.-H. Wu. Electrochemical potential of intercalation phase: Li/ $V_2O_5$  system. *Appl. Surf. Sci.* 253 (2006) 1713.
6. Q.-H. Wu, A. Thissen, W. Jaegermann. Photoelectron spectroscopic study of Na intercalation into  $V_2O_5$  thin films. *Solid State Ionics* 167 (2004) 155.
7. J. Zheng et al. New strategy for the morphology-controlled synthesis of  $V_2O_5$  microcrystals with enhanced capacitance as battery-type supercapacitor electrodes. *Cryst. Growth Des.* 18 (2018) 5365.
8. Y. Wang et al. Self-templating synthesis of double-wall shelled vanadium oxide hollow microspheres for high-performance lithium-ion batteries. *J. Mater. Chem. A* 6 (2018) 6792.
9. D.-W. Han et al. Effects of Fe doping on the electrochemical performance of  $LiCoPO_4/C$  composites for high power-density cathode materials. *Electrochemistry Communications* 11 (2009) 137.
10. H.H. Li et al. Fast synthesis of core-shell  $LiCoPO_4/C$  nanocomposite via microwave heating and its electrochemical Li intercalation performances. *Electrochemistry Communications* 11 (2009) 95.
11. A. Eftekhari. Surface Modification of Thin-Film Based  $LiCoPO_4$  5 V Cathode with Metal Oxide. *J. Electrochem. Soc.* 151 (2004) A1456.
12. K. Hammoum et al. Optical emissions of products sputtered from Fe,  $Fe_2O_3$  and  $Fe_3O_4$  powders. *Eur. Phys. J. D* 61 (2011) 469.
13. C.S. Lee, T.M. Yen, J.H. Lin. Light emission from an oxygen covered copper surface by ion bombardment. *Surf. Sci.* 488 (2001) 379.
14. A. El Boujlaidi et al. Continuum radiation emitted from transition metals under ion bombardment. *Eur. Phys. J. D* 66 (2012) 273.
15. M. Ait El Fqih et al. On the validity of the electron transfer model in photon emission from ion bombarded vanadium surfaces. *Eur. Phys. J. D* 63 (2011) 97.
16. M. Benmoussa et al. Structural, Optical and Electrochromic Properties of Sol-Gel  $V_2O_5$  Thin Films. *Active and Passive Elec. Comp.* 26(4) (2003) 245.
17. A. Afkir et al. Angular distribution of particles sputtered from a copper target by 5-keV Kr ions: Experiment and simulation study. *Surface and Interface Analysis* 53(9) (2021) 792.
18. M. Ait El Fqih, P.-G. Fournier. Ion beam sputtering monitored by optical spectroscopy. *Acta Physica Polonica A* 115(5) (2009) 901.
19. M. Ait El Fqih, P.-G. Fournier. Optical emission from Be, Cu and CuBe targets during ion beam sputtering. *Nucl. Instrum. Methods B* 267 (2009) 1206.
20. J. Yao et al. Revitalized interest in vanadium pentoxide as cathode material for lithium-ion batteries and beyond. *Energy Storage Materials* 11 (2018) 205.
21. L. Jadoual et al. Ion-photon emission from titanium target under ion beam sputtering. *Nucl. Phys. At. Energy* 22 (2021) 358.
22. H.D. Hagstrum. Ion-Neutralization Spectroscopy of Solids and Solid Surfaces. *Phys. Rev.* 150 (1966) 495.
23. A.A. Radzig, B.M. Smirnov. *Reference Data on Atoms, Molecules, and Ions* (Berlin, Heidelberg: Springer-Verlag, 1985) 466 p.
24. W.F. van der Weg, E. Lugujo. Bombardment-induced photon emission from solids. In: *Atomic Collisions in Solids*. S. Datz, B.R. Appleton, C.D. Moak (Eds.). Vol. 2 (New York: Springer, 1975) p. 511.
25. T.S. Kiyani, V.V. Gritsyna, Ya.M. Fogel. On the continuous spectrum emitted by particles ejected from the surface of solid targets by an ion beam. *Nucl. Instrum. Meth.* 132 (1976) 415.
26. C.W. White et al. Continuum optical radiation produced by low-energy heavy particle bombardment of metal targets. *Nucl. Instr. Methods* 132 (1976) 419.
27. C.B. Kerkdijk et al. Continuum photon emission by some metals under heavy ion bombardment. *Nucl. Instr. Methods* 132 (1976) 427.
28. E.O. Rausch, A.I. Bazhin, E.W. Thomas. On the origin of broad band optical emission from Mo, Nb, and W bombarded by heavy ions. *J. Chem. Phys.* 65 (1976) 4447.
29. E. Veje. Accelerator-based chemiluminescence from steady-state gas-surface reactions. *Vacuum* 39 (1989) 429.
30. A.I. Bazhin, M. Suchanska, S.V. Teplov. Model of continuum optical radiation induced by ion bombardment of metals. *Nucl. Instrum. Meth. B* 48 (1990) 639.
31. I.S.T. Tsong. Photon emission from sputtered particles during ion bombardment. *Phys. Stat. Sol. (a)* 7 (1971) 451.
32. I. Terzić, B. Perović. Spectral analysis of light emitted from metallic targets bombarded by high energy ions. *Surf. Sci.* 21 (1970) 86.
33. R.V. Stuart, G.K. Wehner. Sputtering Thresholds and Displacement Energies. *Phys. Rev. Lett.* 4 (1960) 409.
34. H. Kerkow. Photon Emission during Bombardment of Solids with Alkali Ions in the Energy Range between 2 and 10 keV. *Phys. Stat. Sol. (a)* 10 (1972) 501.
35. K. Jensen, E. Veje. An experimental study of optical radiation from sputtered species. *Z. Physik* 269 (1974) 293.

К. Бріа<sup>1</sup>, М. Айт Ель Фкіх<sup>1\*</sup>, Р. Журдані<sup>2</sup>, Л. Жадуаль<sup>2</sup>, А. Каддурі<sup>2</sup>

<sup>1</sup>Лабораторія штучного інтелекту та інженерії складних систем,  
Університет Хасана II Касабланки, Касабланка, Марокко

<sup>2</sup>Лабораторія матеріалів, енергії та навколишнього середовища, Університет Каді Аїяд,  
Марракеш, Марокко

\*Відповідальний автор: m.aitelfqih@gmail.com

### ВПЛИВ ДОДАВАННЯ ЛІТІУ В ТОНКІ ПЛІВКИ ПЕНТОКСИДУ ВАНАДІЮ. ДОСЛІДЖЕННЯ НЕПЕРЕРВНОГО ВИПРОМІНЮВАННЯ

Досліджено оптичне випромінювання  $\text{Li}_{x(x=0,2,0,7,1,2)}\text{V}_2\text{O}_5$  під час бомбардування іонами  $\text{Kr}^+$  з енергією 5 кеВ. Неперервна люмінесценція спостерігалася в широкому діапазоні довжин хвиль від 280 до 340 нм. Як правило, на інтенсивність випромінювання впливала кількість літію, що викликало перехідні ефекти, а також збільшення інтенсивності ліній. Експериментальні результати свідчать про те, що неперервне випромінювання залежить від характеру поверхневої взаємодії між літієм і пентоксидом ванадію і, ймовірно, пов'язане з його електронною структурою.

*Ключові слова:* наплення, золь-гель, оптична емісія, пентоксид ванадію, інтеркаляція і деінтеркаляція.

Надійшла/Received 11.11.2022